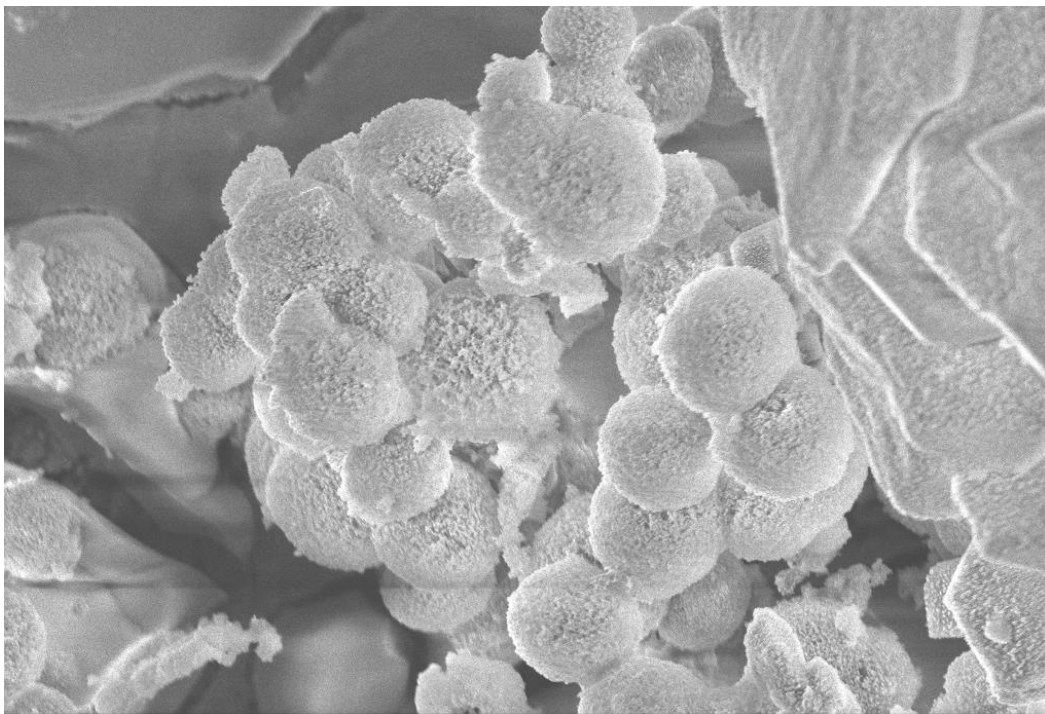


# CHALMERS



## Microcapsules for controlled release of antimicrobials to chronic wounds

---



*Master of Science Thesis*

**Mona Amiri**

Department of Chemical and Biological Engineering  
Division of Applied Surface Chemistry  
CHALMERS UNIVERSITY OF TECHNOLOGY  
Göteborg, Sweden, 2013

Report no.

## Table of Contents

Summary .....	
1. Introduction/background.....	1
1.1. Aim.....	2
2. Theory .....	4
2.1. Layer by layer technique .....	4
2.2. Polyelectrolyte / polypeptide.....	5
2.3. Betaine ester .....	8
2.4. Polyhexamethylene biguanide hydrochloride, PHMB.....	9
2.5. Staphylococcus aureus, V8 Glutamyl endopeptides .....	9
2.6. SEM/ESEM.....	9
2.7. Confocal laser scanning microscopy CLSM.....	10
3. Experimental and methods.....	12
3.1. Layer-by-layer assembly of PLGA/PLL capsules.....	12
3.1.1. Preparation of PLL and PLGA solutions .....	12
3.2. Layer-by-layer assembly of PAA/polyDADMAC capsules .....	13
3.2.1. Preparation of PAA and PolyDADMAC solutions.....	13
3.3. Adsorption of PHMB on Vasolipid surface .....	14
3.3.1. Preparation of Vasolipid and PHMB solutions .....	14
3.4. Layer-by-layer assembly of PAH and PLGA for production of hallow capsules .....	14
3.4.1. Capsules preparation .....	14
3.4.2. To remove CaCO <sub>3</sub> core.....	15
3.4.3. Crosslinking of the hollow capsules.....	15
3.4.4. Loading of the hollow capsules with FITC-dextran.....	16
3.5. Light microscope .....	16
3.6. Microelectromikrophoresis and zeta potential measurement .....	16
3.7. SEM measurement.....	17
3.8. ESEM measurement .....	17
3.9. CLSM measurement.....	17
4. Results.....	19
4.1. PLGA/PLL capsules multilayer.....	19
4.1.1. Light microscope.....	19
4.1.2. Zeta-potential measurement .....	19

4.1.3.	ESEM measurement .....	21
4.2.	PAA/polyDADMAC capsules multilayer .....	21
4.2.1.	Light microscopy.....	21
4.3.	PHMB adsorption on Vasolipid capsules surface .....	23
4.3.1.	Light microscopy.....	23
4.3.2.	Zeta-potential .....	24
4.4.	Production of hollow multilayers capsules and loading them with FITC-dextran....	25
4.4.1.	Light microscopy.....	25
4.4.2.	Zeta-potential measurement .....	27
4.4.3.	ESEM images .....	28
4.4.4.	SEM images .....	28
4.4.5.	CLSM investigates .....	30
5.	Discussion .....	32
6.	Future work.....	36
7.	Acknowledgement .....	37
	References .....	38

## Summary

One definition of chronic wound is “those not following normal wound healing trajectory” but another more common definition is “ulcers (wounds) older than 3 months of age”. However, the number of chronic wounds is increasing worldwide with the number of lifestyle disease patients.

The growth of bacterial biofilms in chronic wounds can explain the characteristics of the chronic wounds and why they do not heal despite different treatments. Antibiotic treatment in cases where biofilm is formed and is growing will provide temporary relief on both the inflammation and the healing. The bacteria in biofilm are less receptive to antibiotics than bacteria positioned outside the biofilm. In addition, the antibiotics may be able to stimulate biofilm capable bacteria and strengthen their resistance against antibiotics.

To eliminate the factors that prevent healing, the wound-bed preparation is decisive. The target is to maximize the effect of wound care and thus promote healing. One solution to prevent risk of bacterial resistance is a more exact dose of antimicrobials locally to the wound, “intelligent” drug delivery, when it shows signs of infection. The aim of this project is to create and study capsules based on PLGA and PLL using the LbL assembly technique. Both polypeptides are biocompatible and highly biodegradable, properties that have made them of interest for use in biomaterial claims. The enzyme V8 (glutamyl endopeptidase) is expected to break down the capsules multilayer and thus release an active substance, in this case betaine ester, which was dissolved in an oil phase in the core.

Another study was done in this project, producing hollow capsules by using  $\text{CaCO}_3$  templates. Multilayers of PAH and PLGA were built up on  $\text{CaCO}_3$  templates and then crosslinked before removal of the template by dissolution and the following loading of an active substance in the hollow core.

The capsules were studied using the following techniques and instruments: light microscopy, microelectrophoresis, ESEM, SEM and CLSM.



## 1. Introduction/background

The term "chronic wound" is more common today; however, yet there are still different definitions of what the term signifies. One definition is "those not following normal wound healing trajectory" (1) and another more common definition is "ulcers (wounds) older than 3 months of age" (1) One to two percent of people in industrialized countries will experience a chronic wound during their lifetime (Gottrup 2004). The number of lifestyle diseases, such as diabetes, heart- and blood diseases and obesity, are on the rise worldwide, which in turn cause an increase in chronic wounds. An estimate of 246 millions are believed to suffer from diabetes worldwide and this figure is expected to increase to 380 million by the year of 2025 (Diabetes Atlas) (1).

A chronic wound can be the first symptom of diabetes. 15 percent of people with diabetes will experience lower extremity ulcers and 14-24% will experience lower extremity ulcer that leads to amputation (ADA). Wounds are often treated by controlling ischemia, off-loading, compression therapy and ambulation. Antibiotics are used when the wound is infected (1). The pH of the chronic wound is in the range of 7.15-8.9, a figure that moves towards neutral pH and even acidic pH during healing (2).

Wound microbiology is divided into three levels: first, contamination which implies that bacteria are presence in the wound but not growing; second, colonization where bacteria are growing in the wound but not causing any infection or tissue damage; and finally, infection where bacteria causes tissue damage and thus infection in the wound. Bacteria normally play a helpful role in wound healing. But the effect of harmful bacteria, such as *Clostridium perfringes* and *Streptococcus pyogenes*, which are less common in human skin microflora is discovered. *Staphylococcus aureus* is a common member of human microflora but may also cause wound infection. When an acute infection is advancing, cleansing, dressings and antibiotic therapy are often effective treatments to kill and inhibit the bacterial growth and activate the immune system to clear the infection (1).

In vivo studies (3) (4) (5) (6) show that bacteria form biofilms rapidly in chronic infected wounds in animal models. James et al studied biofilm presence in 50 specimens from chronic wounds and 16 from acute wounds (7). They found biofilms in 60% of the chronic wounds and 6% of the acute wounds (1).

The growth of bacterial biofilms can explain the characteristics of the chronic wounds and why they do not heal despite different treatments. The bacterial biofilm disrupts the human immune system and facilitates the formation of more bacterial communities, which results in inflammation of the chronic wounds and prevents healing. Antibiotic treatment in cases where biofilm is forming and growing will only provide temporary relief on both the inflammation and the healing. Bacteria in protective biofilm are not very susceptible to antibiotics. In addition the antibiotics may even stimulate biofilm producing bacteria and strengthen their resistance against antibiotics (1).

To eliminate or remove the factors that prevent healing, the wound-bed preparation is decisive. The goal is to maximize the effect of the wound treatment and thus promote healing. The primary role of the wound dressing is to keep moisture balance through the absorption of exudate through the first layer and retain the liquid in the following wound dressing layers (1). A secondary function of the wound dressing can be to release active substances into the chronic wound (8).

One solution for preventing bacterial resistance is to distribute a more exact dose of antimicrobials locally to the wound when it shows signs of infection. Controlled release of active substances created by self-assembled thin film techniques has become more popular (8). “Intelligent” drug delivery would be a great solution to prevent unnecessary exposure of drugs to the patient, thus avoiding unwanted side effects. Using the layer-by-layer technique (LbL) to create nanofilms based on polypeptides for release of antimicrobials has been studied and fabricated before (8). Thus, the next step was to apply the film-forming knowledge to create capsules based on polypeptides for controlled release of antimicrobials.

This diploma work is a part of a PhD project at Mölnlycke Health Care AB and SuMo Biomaterials (Vinn Excellence Center). Most of the laboratory work is performed at Chalmers.

## 1.1. Aim

The aim of this project was to study and produce capsules consisting of polypeptides that can release active substances. Cationic and anionic polypeptides, poly-L-glutamic acid (PLGA) and pol-L-lysine (PLL), adsorb to one another at pH=7.4, using the LbL assembly technique. One of the chosen active substances, betaine ester, a cationic antimicrobial, is dissolved in an oil phase and is placed in the core of the capsules by forming an o/w emulsion. Another cationic antimicrobial, PHMB, is supposed to be loaded in the core of multilayer capsules produced by template assisted assembly. A protease from *S. aureus*, V8 (glutamyl



endopeptidase), that is common in infected and critically colonized wounds, causes beak-down of the multilayers (8) and should thus release the active substance to the infected wound.

PLL and PLGA have been found to be useful for this purpose due to their ability to grow multilayers film in an exponential manner. The electrostatic attraction between lysine's- and glutamic acid's side chains is the main momentum of the self-assembly (9). Both polypeptides are biocompatible and highly biodegradable. This property has made them of interest for use in other biomaterials claims (10). Further, the LbL technique presents a good possibility to immobilize and integrate biomacromolecules and other particles such as proteins and dyes (11). Also, PLGA is chosen as the final layer, because studies (12) have demonstrated that PLGA-ending films interact very little with mammalian cells.

This project is expected to contribute to help solve the problem with bacterial resistance and other unwanted side effects of treating an infected chronic wound.

## 2. Theory

The following section will present a brief introduction to the theory, materials and methodology used to carry out this project.

### 2.1. Layer by layer technique

The layer-by-layer (LbL) deposition technique belongs to the same class as template assisted assembly. Self-assembly, or chemical modification cycles, have unclear final results and are usually slower than the LbL deposition technique. An advantage with the LbL deposition is its ability to build complex multilayer films without any chemical modifications. Also, the LbL process is an environmentally friendly and inexpensive technique that fabricates functional multicomposite films (13).

The LbL technique relies on ionic surface charges and their interaction with counterions. Figure 1 illustrates how inorganic and organic polyelectrolytes are exposed to oppositely charged building blocks after every washing step, forming inorganic and organic multilayer materials. The surface charge overcompensation occurs when positively- and negatively charged surfaces are deposited in a step by step process. Zeta potential measurements show the excess charge after each deposited layer (14).

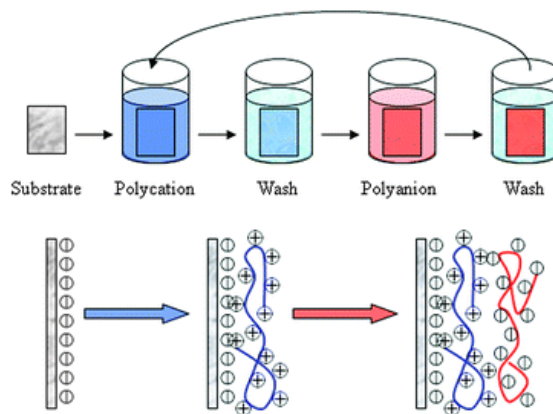


**Figure 1: The first two adsorption steps in LbL deposition, which explains the film formation. The substrate in the figure is negatively charged (44).**

Each layer in a multilayer film has individual structures and properties dependent on the arrangement of the molecules. Each layer is not purely cationic or anionic, but the polyelectrolytes intermingle throughout the film. Therefore, one layer is normally defined as an average across a certain area (13).

There are many interactions in a multilayer film, such as donor/acceptor interactions, hydrogen bonding, adsorption/drying cycles, covalent bonds, stereocomplex formation or specific recognition needed between two species “reagents” for multilayer deposition (13).

One of the most important properties of a single layer is its thickness, which is reliant on the properties of the underlying surface, *e.g.* density, nature, charged groups, their local agility and the surface smoothness. Important properties during film assembly include deposition conditions, solvent, temperature, salt concentration, concentration of adsorbing species, adsorption time, washing time, humidity, *etc.* (13).

## 2.2. Polyelectrolytes / polypeptides

Polymers with either positively or negatively charged ionizable groups are called polyelectrolytes. The polymer chains are in solution, particularly in polar solvents, surrounded by counterions, which are connected to each ionizable group (15).

There is also electrostatic interactions between the ionizable groups in the polyelectrolyte chain, which causes a greater strain of the chain than it does in an uncharged polymer. Hence, the viscosity is different for polyelectrolyte solutions compared to solutions containing an uncharged polymer. This can further be explained by that the viscosities for polyelectrolyte solutions are proportional to the square root of the polymer concentration for the polyelectrolyte solution, whereas the viscosity of the uncharged polymer solution is proportional to the polymer concentration in the same concentration (15).

The interaction between the adsorbing substrate and polyelectrolyte chains controls the local polymer concentration. The diluted solution of the adsorbed chains becomes a two-dimensional semi-dilute solution when the concentration of the surface charges increases. If the surface charge continues to be denser than the adsorbed polyelectrolyte layer, the polyelectrolyte chains will accumulate around the surface, which in turn will increase the thickness of the adsorbed film (15).

Poly diallyldimethylammonium chloride, polyDADMAC, is a synthesized linear polymer with high cationic charge density. This polymer is able to attract the negatively charged functional groups to surfaces by coating and modifying the surface. One application of this polymer is for water purification (16) (17).

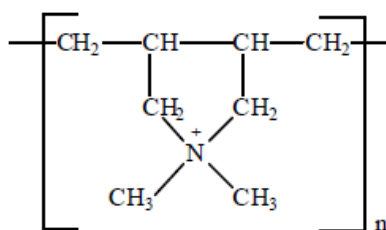


**Figure 2: PolyDADMAC molecule structure (16).**

Polyacrylic acid, PAA, is a weak anionic polyelectrolyte, which can form gels with organic solvents or water. The monomers in the PAA polymer chains are connected by crosslinking between the carboxyl groups. In the presence of some solvent, the intramolecular structure is broken due to the neutralization of the acidic groups, which leads to the formation of a gel. PAA and its derivatives can swell up to 1000 times. At a low pH value, PAA is deprotonated in water and the conformation of the polymer is due to the strong intramolecular hydrogen bonding. At high pH, the charge density increases and the polymer conformation depends on electrostatic repulsion (18).

PAA based gels are used in, *e.g.* drug delivery, for synthesis of nanoparticles by sol-gel method and as a cleansing agent (19).

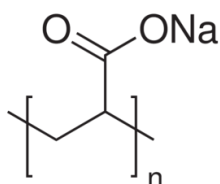


**Figure 3: Molecule structure of Polyacrylic acid sodium salt (PAA) (40).**

Polypeptides are polymers consisting of amino acids as their monomeric groups. The amino acids are organic compounds made from an acid group and an amine group, where the amine group is attached to the  $\alpha$ -carbon atom. When a carboxyl group reacts with an amine group, the bond formed is called peptide bond or amide bond, which is planar. If water is eliminated from the amino acids then polypeptides are produced. . Peptides are responsible for some of the basic mechanisms of human biological processes, such as the processes involving enzymes, hormones or antibodies (20) (21).

Poly- L- glutamic acid, PLGA, is made of naturally occurring L-glutamic acid. These L-glutamic acid monomers are connected with degradable amide bonds, thus making PLGA

biodegradable and nontoxic. These properties make PLGA a promising choice as a polymer involved in-drug release (22).

PLGA is an anionic polypeptide and due to the electrostatic repulsion between the negatively charged cell surface and the polymer, the cellular uptake of the polymer is hindered (22).

The carboxylate groups in the polymer are the functional parts. At a neutral pH, the  $\gamma$ -carboxyl group in every repeating unit is negatively charged, making PLGA water soluble (22). At  $\text{pH} > 5$ , the charge density increases and PLGA has a random coil form. At  $\text{pH} < 5$ , the charge density decreases and the polymer gets a more rod-like shape. Consequently, the degradation rate of PLGA is affected by changing pH (22).

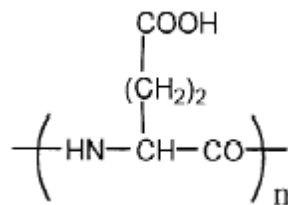


**Figure 4: Molecular structure of PLGA (22).**

Poly- L- lysine, PLL, is a cationic biocompatible polymer with abundant amino groups. PLL is useful in drug delivery and even for cell adhesion. Other applications for PLL are for biofuel cells and DNA electrochemical sensors. Good solubility in water, good biocompatibility, abundant active amino groups and elastic molecular backbone has made PLL a useful polyelectrolyte for many applications (23).

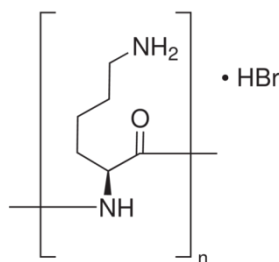


**Figure 5: Molecular structure of PLL (41).**

Polyallylamine hydrochloride, PAH, is a weak cationic bio-mimicking polymer with  $\text{NH}_2$  as functional group. PAH gives products with different properties when exposed to different pH and with time (ageing) (24).

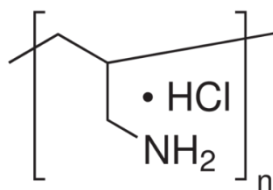


Figure 6: Molecule structure of PAH (42).

### 2.3. Betaine ester

Betaine is a carboxylic acid produced from natural metabolic oxidation of choline (25). Esterified betaine is antimicrobially active and belongs to the group of quaternary ammonium compounds (QACs). Betaine ester is esterified from fatty alcohols with hydrocarbon chain lengths of 10-18 carbon atoms (26). Amphiphilic quaternary ammonium compounds are known to be prompt disinfectors for different applications. They bind to biological membranes with their cationic surface and may kill the organism by penetrating the membrane and causing an outflow of intracellular material. After causing a cell membrane to rupture, they degrade into components with low toxicity, hence minimizing the environmental damages. This property puts betaine esters in the category of “soft” QACs (25). The carbonyl atom is electron deficient due to the positively charged nitrogen atom, making the function of the ester sensitive to hydroxide ions and thus hydrolysis (27).

The ester hydrolyses quicker at higher pH. The hydrolysis rate was 90% in less than 10 minutes at 30°C and pH=9, but only 10 % at pH=6 after 18 hours (26). In other words, pH, temperature, concentration, molarity of the buffer, chain length of the compound, type of anion and effect from biological matters as proteins, all affect the hydrolysis rate (28). Betaine and fatty alcohol are the hydrolysis products (see figure 7) and they are natural metabolites (25).

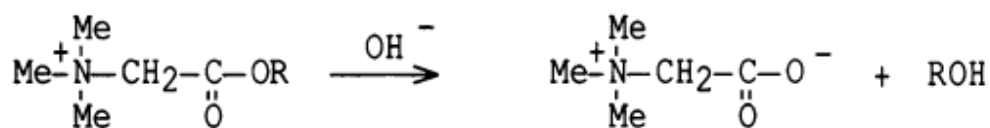


Figure 7: Hydrolysis of betaine ester (26).

Betaine ester may replace other more stable compounds in antiseptic applications that are in use now, due to their quick killing effect and their degradable and non-toxic impact (25).

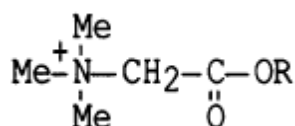


Figure 8: Molecular structure of betaine ester (26).

## 2.4. Polyhexamethylene biguanide hydrochloride, PHMB

PHMB is a white to yellow powder or an aqueous solution, and is used as a preservative, sanitizer or disinfectant. For sanitization and disinfection, PHMB is used to kill bacteria and viruses in *e.g.* wound irrigation and dressings. PHMB is used as a preservative in cosmetics, hand wash and contact lens solutions because of its low toxicity towards mammalian cells (29) (30).

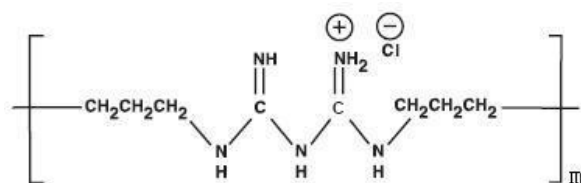


Figure 9: Molecular structure of PHMB (43).

## 2.5. *Staphylococcus aureus* and V8 (glutamyl endopeptidase)

GluV8, also known as V8, is a serine protease in glutamyl endopeptidase I family. This protease assists the growth and existence of *S. aureus* and is an important part in degrading the cell-bound staphylococcus surface adhesion molecule. V8 is able to rapidly cleave peptide bonds, especially glutamic acid and weak aspartic acid bonds. The nucleotide tail codes a protein with 336 amino acids (31).

V8 activity is dependent on two ionizable groups with pK<sub>a</sub> values of 5.8 and 8.4. The optimum pH for V8 is shown to be 8, with chromogenic substrates (32).

## 2.6. SEM/ESEM

SEM stands for Scanning Electron Microscopy and is a microscope using an electron beam produced at the top of the microscope by an electron gun. It is used for studying the surface of materials. The electron beam goes down through the microscope, which is kept in vacuum, then through the electromagnetic field and the lens, which focuses the beam towards the sample (see figure 10). Electrons and X-rays are produced when the beam hits the sample (see figure 11). A detector gathers backscattered and secondary electrons and converts them into

signals that are sent to a screen, which shows a 3D reconstruction of the surface morphology (33) (34)

When using SEM, a large part of the specimen can be in focus, since SEM has a large depth of field. SEM uses electromagnetics rather than lenses and makes it possible to control the magnification, which enables very high resolution images, *i.e.* up to 1nm (33) (34).

All samples should be dry when used in SEM, since the water would vaporize in the vacuum. All non-conductive samples, such as non-metals, should be made conductive by covering the surface with a thin layer of conductive material, *e.g.* gold. This can be done in a so-called sputter coater. (34)

ESEM stands for environmental scanning electron microscopy and creates images similar to SEM. The great advantage of ESEM over SEM is its ability to produce high resolution images of specimen in its “natural” state, namely moisture containing and non-conductive samples, *e.g.* biological materials which otherwise are difficult to place in vacuum (35).

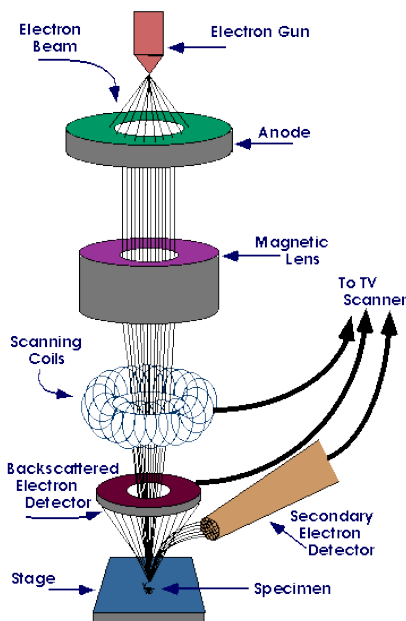


Figure 11: SEM (34).

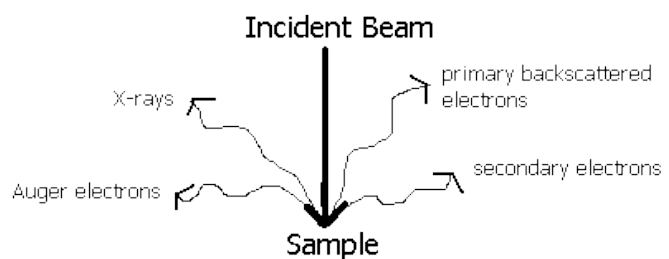


Figure 10: How the electron beam hits the sample surface and produces different electrons (34).

## 2.7. Confocal laser scanning microscopy CLSM

Confocal laser scanning microscopy, CLSM, is a rather new technique for studying biological structures and food items. In comparison with conventional light microscope, the light source is exchanged for a laser, a scanning part and a pinhole, to develop the limitation of the depth



and focus. CLSM produces optical sections in a 3D sample by moving the focal plane in certain steps ( $\mu\text{m}$ -range) through the depth of the sample (36).

Further, CLSM uses a collimated polarized laser beam that is deflected gradually in the x- and y-directions by a scanning part, before reflection by a dichroic mirror, which creates an image of the sample. The wavelength of the fluorescent light emitted through the sample is dependent on which fluorescent dye that is used. The light is then gathered by a lens and passed through the dichroic mirror. Then, in order to eliminate out-of-focus light, these wavelengths are focused into a small pinhole. A light-sensitive detector, placed behind the confocal opening, registers the in-focus information of every point of the sample. The output is digitized signals to a computer, which creates an image (36).

A great advantage with CLSM is the possibility to change the surrounding environment of the sample, such as cooling, heating, mixing, and follow the changes *in situ* (36). However, most samples need to be prepared for visibility in the CLSM before use. These steps, *e.g.* staining, need to be done in a liquid and often at room temperature, a process which can destroy the sample, either by swelling or solubilization. Also, many components are sensitive to the exposure of laser light, which can bleach the sample over time (36).

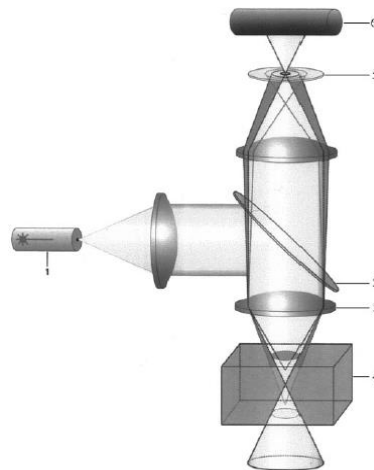


**Figure 12: Principal of CLSM. (1) laser, (2) dichroic mirror, (3) objective lens, (4) sample, (5) confocal pinhole, (6) photomultiplier (36).**

### 3. Experimental and methods

In the following section the preparation of materials and methodology is described in detail.

#### 3.1. Layer-by-layer assembly of PLGA/PLL capsules

The preparation of PLGA and PLL for producing o/w emulsion capsules with betaine ester in the core is described below.

##### 3.1.1. Preparation of PLL and PLGA solutions

0.1 wt% betaine ester (synthesized and provided by Dr. Dan Lundberg, Lund University) was added to the oil phase, glyceryl trioctanoate, purchased from Sigma-Aldrich. They were left on a magnetic stirrer for about 1 h or until all the betain ester was dissolved in the oil phase.

Poly-L-lysine (PLL), MW=30-70 kDa, Cas no. 25988-63-0, and poly-L-glutamic-acid (PLGA), MW=50-100 kDa, Cas no. 26247-79-0, were purchased from Sigma-Aldrich and they were used as received. A 0.1mM buffer solution from Tris-HCl (Sigma) and Milli-Q water (resistivity  $\geq 18 \text{ M}\Omega \text{ cm}$ , 25°C) was prepared. 0.1M NaCl (Fluka) was added to the buffer solution. Both PLL and PLGA were prepared in an amount corresponding to 1 mg/mL, respectively. The final solution was left on a magnetic stirrer for 1 h before use. The pH was 7.4 for the final solutions.

The PLGA solution was transferred to a round beaker placed in a water bath to keep the temperature of the solution around room temperature during mixing. A mixer was put in the solution at a speed of 5000 rpm. Then, the betaine ester dissolved in the oil phase was added in drops to the PLGA solution. When adding the oil phase to the polypeptide solution, the final solution became turbid and white as milk, indicating that an emulsion had been formed. As a final step the mixing rate was increased to 10.000 rpm and the solution was left for exactly 1 h.

The emulsion was now prepared and thus emptied into a glass bottle with a lid and placed on a magnetic stirrer. The emulsion should stand on the magnetic stirrer all the time for the stability of the o/w spheres.

The emulsion was centrifuged for 1.5 hours at 10.000 rpm with a high speed centrifuge of model Beckman. The residual non adsorbed polyelectrolyte was removed by washing once and then the emulsion was diluted into its original volume. The washed and diluted solution was put on a magnetic stirrer and the PLL solution was added drop-wise. Then the final

solution was left on a magnetic stirrer for about 20 minutes for further adsorption. The same procedure was applied for centrifugation and washing as previously described, now containing one PLGA layer and one PLL layer. The next and the last PLGA- layer was added and the solution was centrifuged, washed and diluted yet again. Thus the final spheres, or “capsules”, contained an oil core with betaine ester and three layers as shell, *i.e.* PLGA/PLL/PLGA.

### **3.2. Layer-by-layer assembly of PAA/polyDADMAC capsules**

The preparation of PAA and polyDADMAC for producing of capsules with betaine ester in the core is described below

#### **3.2.1. Preparation of PAA and PolyDADMAC solutions**

Due to the high cost of the PLGA and PLL, poly(acrylic) acid.NaCl (PAA) and poly diallyldimethylammonium chloride (polyDADMAC) was used as model polyelectrolytes. They are both synthetic polyelectrolytes and were used in varying concentrations.

PAA, MW=225 kDa, Cas no. 9003-04-7, was purchased from Polyscience as a 20% aqueous solution. PolyDADMAC, MW=300 kDa, Cas no. 26062-79-3, was purchased from Akzo Nobel as a 40% aqueous solution. As PLGA and PLL, these two polyelectrolytes were used as received. 0.1M and 1M NaCl solutions in Milli-Q water was prepared, and PAA or polyDADMAC was added in an amount corresponding to 1 mg/mL or 10 mg/mL, respectively. The solution was left on a magnetic stirrer for 1 h. 0.1 wt% betaine ester was dissolved in glyceryl trioctanoate (as previously described) and added to the PAA solution in a drop-wise manner (see the previous section). Three different oil/water ratios were studied, 16.67%, 40% and 50%.

Cholesterol, MW=386.65 g/mol, Cas no. 57-88-5, was purchased from Sigma-Aldrich and was used to study if cholesterol would have any effect on stabilizing the core. Different amounts of cholesterol were examined, *i.e.* 0.3 wt%, 0.6 wt% and 1.2 wt%. The cholesterol was added to the oil phase after betaine ester had dissolved in the oil phase. Also, the pH value was adjusted to 5 (37) for PAA and polyDADMAC by HCl for some samples to study if pH had an effect on the capsules' stability.

The solution was filtered and the excess polyelectrolytes were removed by washing twenty times and diluted into the original volume using a membrane filter of model Micon with pore

sizes 100 KDa and 300 KDa (Millipore). As the driving force for the filtration, nitrogen gas of 2 bar was used.

PolyDADMAC and PAA layers were adsorbed, respectively, to the washed and diluted solution while it was standing on a magnetic stirrer until three layers had been assembled.

### **3.3. Adsorption of PHMB on Vasolipid surface**

In the section below, the preparation of Vasolipid and PHMB for adsorption of PHMB on Vasolipid capsules is described

#### **3.3.1. Preparation of Vasolipid and PHMB solutions**

Vasolipid (triglyceride emulsion) was purchased from the drug store, Apoteket Hjärtan. Polyhexamethylene biguanide hydrochloride, PHMB, was purchased from Arch Chemical UK, and was received as a 20 % aqueous solution called Cosmocil. 0.4% aqueous solution of PHMB was prepared with Milli-Q water and added to the Vasolipid on magnetic stirrer, in a ratio of 1:1. The emulsion was left for about 20 minutes for further adsorption of PHMB to the Vasolipid “capsule” surface. The emulsion was then centrifuged with a high speed centrifuge at 10.000 rpm for 1.5h. The emulsion was washed twice to remove excess polyelectrolyte, and diluted into its original volume.

A 1mg/mL PLGA solution containing 0.1mM Tris-HCl and 0.1M NaCl was prepared, in the same manner as mentioned in section 3.1.1. The PLGA solution was placed on a magnetic stirrer and the PHMB / Vasolipid emulsion was added drop-wise and left for adsorption for 20 minutes.

### **3.4. Layer-by-layer assembly of PAH and PLGA for production of hollow capsules**

The preparation of PAH, PLGA and PLL for production of hollow capsules with CaCO<sub>3</sub> as the sacrificial template core, is described below.

#### **3.4.1. Capsules preparation**

Calcium carbonate capsules, with an average size of 3µm, was purchased from Plasma Chem, Germany. CaCO<sub>3</sub> was used as a sacrificial template for preparation of capsules as follows. A 0.1mM buffer solution with Tris-HCl and Milli-Q water was prepared. 0.15M NaCl was added to the buffer solution. Poly (allylamine hydrochloride), MW=900 kDa, Cas no. 71550-12-4, purchased from Sigma-Aldrich was added in an amount corresponding to 2mg/mL. The

polyelectrolyte solution was adjusted to 6.5 by either HCl or NaOH. 2 wt% CaCO<sub>3</sub> was weighed and added to the polyelectrolyte solution. The solution was shaken rapidly several times to avoid aggregation of the CaCO<sub>3</sub> spheres and to allow adsorption of the polyelectrolytes to the CaCO<sub>3</sub> surface. The solution was left on a magnetic stirrer for 20 minutes. Then, the solution was sonicated for few seconds. They were centrifuged later and washed four times, 5 minutes and 3500 rpm every time, using a centrifuge of model Labofuge 200. An aqueous solution of 0.015M NaCl was used for washing. The capsules were then exposed to a PLGA solution for further film formation and adsorption, which had the same concentration as the PAH solution. For centrifugation and washing, the same procedure as above was repeated. Up to 3 bilayers, with PLGA as ending layer, was built.

Another experiment was carried out with higher polyelectrolyte solution, 4mg/ml. Also the adsorption time was increased from 20 to 30 minutes during PLGA adsorption. The PAH adsorption time was increased to 1 hour, since the PAH polymer seemed to need longer time for surface coverage due to its sheer size.

### **3.4.2. Removal of the CaCO<sub>3</sub> template**

After adsorbing 3 bilayers with PLGA as the ending-layer, the CaCO<sub>3</sub> core was removed. A 0.02M buffer solution was prepared by 4-Morpholineethanesulfonic acid sodium salt (MES) and Milli-Q water, then 4 wt% gluconolactone (GDL) was added while stirring. The capsule suspension was added to the GDL solution and was left on the magnetic stirrer for 30 minutes until the solution became transparent.

### **3.4.3. Partial crosslinking of the hollow capsules**

A covalent bond was formed between the carboxylic group of PLGA and the amine group of PAH by chemical crosslinking. This step was performed by using the water-soluble N-(3-dimethylaminopropyl)-N'-ethylcarbodiimide hydrochloride (EDC) and N-hydroxysulfosuccinimide sodium salt (sulfo-NHS) in 0.15 M NaCl, pH=6.5-7. Two concentrations of EDC were investigated, 50mM and 200 mM, but the concentration of sulfo-NHS was kept constant at 50 mM.

The hollow multilayer capsules were added to the EDC and sulfo-NHS solutions and then stored overnight.

In the next step, a small amount of the PLGA/PLL o/w emulsion from section 3.1.1 was crosslinked by 200mM EDC sulfo-NHS and 0.5M NaCl, for ESEM measurements.

#### 3.4.4. Loading of the hollow capsules with FITC-dextran

Two buffer solutions were prepared, 0.02 M MES, Milli-Q water and 0.15 M NaCl and 0.02M MES, Milli-Q water and 0.5 M NaCl, respectively. FITC-dextran was added in an amount to get a final concentration of 2 mg/mL. The solution was added to the partially crosslinked hollow capsules in a ratio of 2:1.

### 3.5. Light microscope

The PLGA/PLL microcapsules created from the o/w emulsion and the template assisted hollow microcapsules were studied in a light microscope of model BHSM Olympus DP12.

### 3.6. Microelectrophoresis and zeta potential measurement s

A microelectrophoresis instrument (Rank Brothers Ltd, Bottisham) was used to measure the mobility and the surface charge of the capsules. Smoluchowki's equation was used for calculation of the  $\zeta$ -potential:

$$u = (\varepsilon \times \varepsilon_0 \times \zeta) / \rho \quad (1)$$

- $\varepsilon = 80$ , dielectric constant for water at 25°C
- $\varepsilon_0 = 8.85 * 10^{-12} \text{ C}^2/\text{V}^*\text{m}$ , permittivity for vacuum
- $\zeta =$  zeta potential
- $\rho = 0.8 * 10^{-3} \text{ PaS}$ , viscosity of water at 25°C
- $u =$  electrophoresis mobility

$$u = \frac{v}{E} \quad (2)$$

- $v =$  capsule velocity
- $E =$  electric field

$$E = \frac{V}{L} \quad (3)$$

- $V =$  the voltage which was adjusted and kept constant at 100 V
- $L =$  distance between the two electrodes

Washed and diluted samples were added to a 1mM NaCl solution in the ratio 3 $\mu$ L sample to 10mL NaCl solution.

### 3.7. SEM measurement

The following samples were analyzed in a SEM instrument of model LEO Ultra 55 FEG, using electron high tension 5kV with the help of Tina Gschneidtner.

- Hollow capsules cross-linked by 50 mM EDC sulfo-NHS - air dried
- Hollow capsules cross-linked by 200 mM EDC sulfo-NHS - air dried
- Hollow capsules cross-linked by 200 mM EDC sulfo-NHS – freeze dried
- CaCO<sub>3</sub> capsules (*i.e.* with template) cross-linked by 200 mM EDC sulfo-NHS - air dried

All samples were sputtered with gold in a Jeol JFC-1100E Ion Sputter at 10 mA for 90 seconds.

### 3.8. ESEM measurement

The following samples were investigated in an ESEM instrument of model FEI Quanta 200 ESEM FEG (field emission gun) with the help of Lic. Tekn. Anna Jansson. Number of cycles used was 8, the high voltage was set at 5 kV, the maximum pressure was set at 9 Torr and lowered to 4.93 Torr, and the temperature was 1°C. These values were kept constant for all samples; however, the minimum pressure lowered past the water pressure point (4.93Torr) for better visibility of the samples during the measurement.

- The PLGA/ PLL emulsion with 1.5 bilayers, cross-linked with 200 mM EDC sulfo-NHS. The used  $P_{\min}$  was 4 torr.
- CaCO<sub>3</sub> capsules multilayer, non-hollow and non-cross-linked. The used  $P_{\min}$  was 4.5 torr.
- Hollow capsules cross-linked by 200 mM EDC sulfo-NHS. The used  $P_{\min}$  was 4.5 torr.

### 3.9. CLSM measurement

CLSM measurement was performed with the help of Dr. Erich Schuster at SiK<sup>1</sup>, using two CLSM instruments of model LEICA TCS SP5 II and LEICA TCS SP2.

The following samples were investigated:

- Hollow capsules cross-linked by 50 mM EDC sulfo-NHS, loaded by FITC-dextran 0.5M NaCl, at room temperature.

---

<sup>1</sup> SiK- the Swedish Institute for Food and Biotechnology. [www.sik.se](http://www.sik.se)  
Box 5401, SE-402 29 Gothenburg, phone: +46 10 516 66 00, fax: +31 83 37 82 , [info@sik.se](mailto:info@sik.se)

- Hollow capsules cross-linked by 50 mM EDC sulfo-NHS, loaded by FITC-dextran 0.15M NaCl, at room temperature.
- Hollow capsules cross-linked by 200 mM EDC sulfo-NHS, loaded by FITC-dextran 0.5M NaCl, at room temperature.
- Hollow capsules cross-linked by 200 mM EDC sulfo-NHS, loaded by FITC-dextran 0.15M NaCl, at room temperature.
- Hollow capsules cross-linked by 200 mM EDC sulfo-NHS, loaded by FITC-dextran 0.5M NaCl, exposed to V8 enzyme at 32°C.
- Hollow capsules cross-linked by 200 mM EDC sulfo-NHS, loaded by FITC-dextran 0.5M NaCl, exposed to V8 enzyme at 37°C.



## 4. Results

The following sections present the results from formation and analysis of multilayer capsules.

### 4.1. PLGA/PLL multilayer capsules

All results from PLGA/PLL capsules multilayer are presented below.

#### 4.1.1. Light microscope

Figure 13 illustrates an o/w emulsion, with a PLGA/PLL/PLGA multilayer covering the “capsules” The average size of the spheres was between 3  $\mu\text{m}$  to 5  $\mu\text{m}$ . The larger capsules ruptured over time and the oil leaked out.

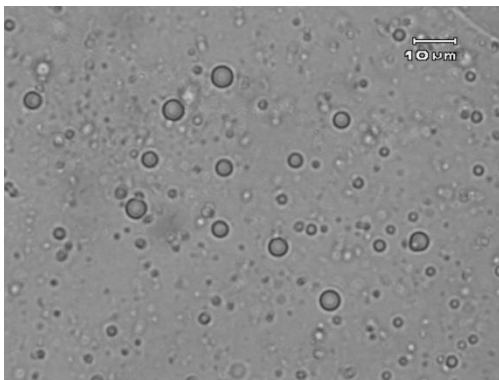


**Figure 13: 0.1 wt% betaine ester in the oil phase (core) with a shell built by polyelectrolytes (PLGA/PLL/PLGA).**

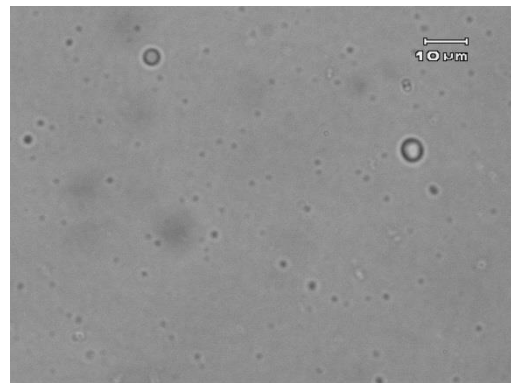


**Figure 14: The same emulsion as Figure 13, but 24 days later**

Figure 14 displays the same emulsion 24 days later. During this time the emulsion was stored on magnetic stirrer with a lid on. Most of the spheres larger than 3  $\mu\text{m}$  had ruptured and the oil had leaked out. This event was also confirmed with the oil layer found above the emulsion. However, the remaining spheres seemed “stable” and remained intact during this project.

#### 4.1.2. Zeta-potential measurements

The zeta-potential was measured after every added layer, before and after washing, and the results are presented in table 1 and in figure 15. These measurements show that the multilayer surface has been charge-overcompensated in each adsorption step, thus promoting adsorption of oppositely charged polyelectrolytes. The capsules’ mobility and also the  $\zeta$ - potential decrease with an increasing number of layers (see table 1). This is probably because of the intermingling of the layers, which allows underlying layers to reach the surface in some spots and therefore affect the surface charge slightly.

**Table 1: Zeta-potential of PLGA/PLL multilayer capsules, 1 mg/mL polyelectrolytes, 0.1M NaCl and 0.1mM Tris-HCl, pH=7.4**

Sample	Washed	Capsules velocity ( $\mu\text{m/s}$ )	Electrophoresis mobility ( $\text{m}^2/\text{V.s}$ )	Zeta-potential (mV)
<b>PLGA 0.1% &amp; 0.1M NaCl</b>	No	66.87	$4.32 \cdot 10^{-8}$	-50.82
<b>PLGA 0.1% &amp; 0.1M NaCl</b>	Yes (centrifugerat x1)	61.46	$3.97 \cdot 10^{-8}$	-44.86
<b>PLGA 0.1% &amp; 0.1M NaCl PLL 0.1% &amp; 0.1M NaCl</b>	No	33.11	$2.14 \cdot 10^{-8}$	+24.17
<b>PLGA 0.1% &amp; 0.1M NaCl PLL 0.1% &amp; 0.1M NaCl</b>	Yes (centrifugerat x1)	30.43	$1.97 \cdot 10^{-8}$	+22.21
<b>PLGA 0.1% &amp; 0.1M NaCl PLL 0.1% &amp; 0.1M NaCl PLGA 0.1% &amp; 0.1M NaCl</b>	No	27.33	$1.77 \cdot 10^{-8}$	-19.95
<b>PLGA 0.1% &amp; 0.1M NaCl PLL 0.1% &amp; 0.1M NaCl PLGA 0.1% &amp; 0.1M NaCl</b>	Yes (centrifugerat x1)	24.66	$1.59 \cdot 10^{-8}$	-18

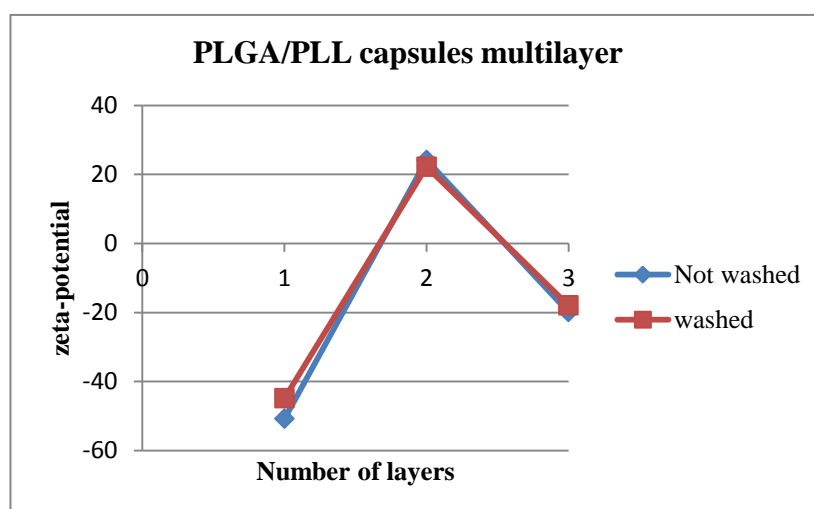


**Figure 15: zeta-potential measurements for PLGA/PLL o/w emulsion spheres or “capsules”.**

### 4.1.3. ESEM measurement

Figure 16 illustrates PLGA/PLL multilayer capsules cross-linked by 200mM EDC and 50mM sulfo-NHS. The white dots in figure 15 are the capsules. As seen in the picture, they are still round even after evaporation of water in the ESEM instrument. This means that the capsules are somewhat more stable when they are cross-linked compare to uncross-linked ones. They withstand evaporation better now, which they did not do before crosslinking

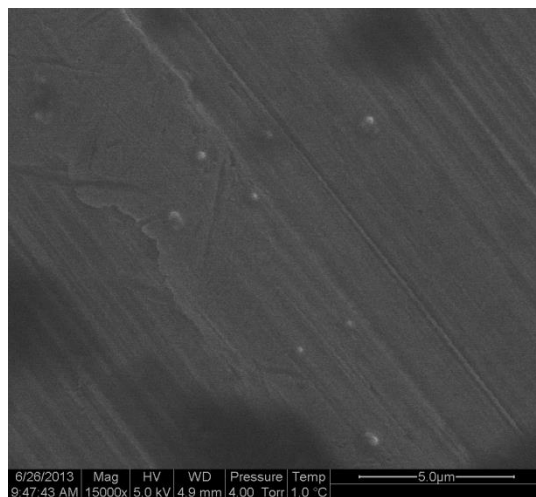


**Figure 16: PLGA/PLL multilayer capsules cross-linked with 200mM EDC and 50mM sulfo-NHS.**

## 4.2. PAA/polyDADMAC multilayer capsules

All results regarding PAA/polyDADMAC multilayer capsules are described below.

### 4.2.1. Light microscopy

Figure 17 demonstrates an o/w emulsion, where the “capsules” have been assembled with PAA and polyDADMAC. The capsules size varied greatly between 2 and 15µm. The capsules aggregated and diffused into each other, meaning that the emulsion was not stable.

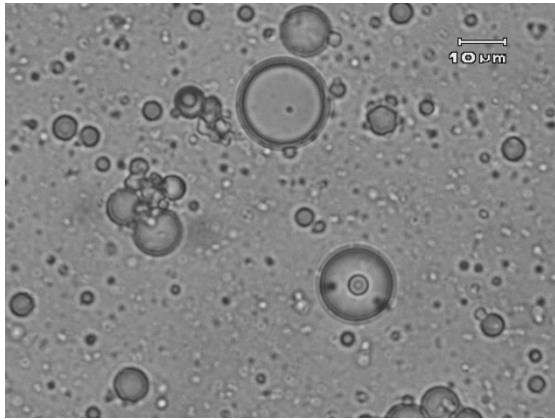


**Figure 18: 0.1 wt% betaine ester dissolved in the oil phase (core), where multilayers constitute the surrounding shell. The polyelectrolytes were assembled at a concentration of 10mg/mL. This picture was taken before filtration.**

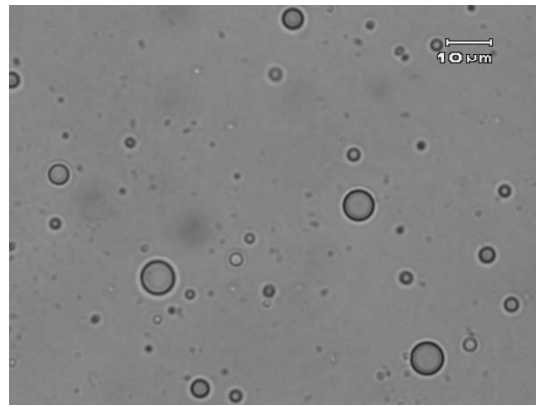


**Figure 17: 0.1 wt% betaine ester in the oil phase, and a multilayer shell. The polyelectrolytes were assembled at a concentration of 1mg/mL, and at pH=5. This picture was taken before filtration.**

When the polyelectrolyte and NaCl concentrations were decreased and pH was adjusted to 5 the emulsion became more stable, see figure 18. PLGA with a pKa at around 5.4 seems to create more stable multilayers at pH= 7.4. However, PAA with a  $pK_a=4.2$  (38), obviously created a more stable emulsion at a lower pH (see Figure 18).

However, despite changing the NaCl concentration, polyelectrolyte concentration, oil/water ratio and pH, the PAA/polyDADMAC emulsion remained rather unstable. The capsules ruptured easily, probably since the average size was larger than capsules in the PLGA/PLL emulsion. When polyDADMAC was added complexes were formed, despite the removal of excess PAA. Filtration caused more disconnection of PAA and thus a collapse of the spherical structure, which is shown in figure 19. This figure illustrates capsules that are not spherical any longer. They were deformed and had small “holes” (darker smaller dots) that had emerged in the capsules. An oil phase was discovered after filtration indicating that the oil phase had leaked out.

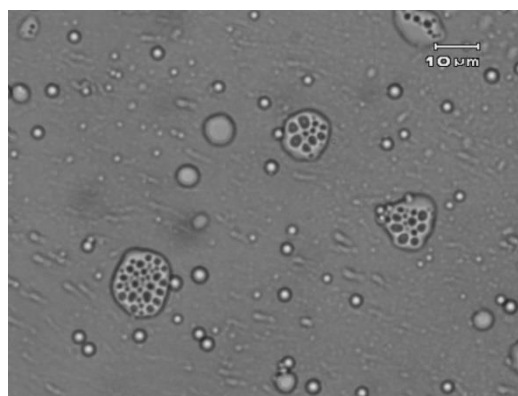


**Figure 19: 0.1 wt% betaine ester dissolved in oil, with PAA/polyDADMAC as the polyelectrolyte shell. Images is taken after filtration.**

#### 4.2.2. Zeta-potential

The results in table 2 show that the electrophoresis mobility and also the  $\zeta$ -potential for the emulsion with PAA was slightly more negatively charged after the emulsion was washed. This value should be less negative after washing due to the removal of excess PAA. This may be due to a slight disconnection of PAA from the glyceryl trioctanoate during filtration. Interaction between polyDADMAC and PAA could therefore be the explanation why complexes were formed after addition of polyDADMAC.

**Table 2: Zeta-potential of PAA/polyDADMAC multilayer capsules. The polyelectrolyte concentration was 10 mg/mL and was pH=5.**

Sample	washed	Capsules velocity ( $\mu\text{m/s}$ )	Electrophoresis mobility ( $\text{m}^2/\text{V.s}$ )	Zeta-potential (mV)
.1 wt% betaine in PAA 1%, pH=5	No	44.15	$2.85 \cdot 10^{-8}$	-32.22
0.1 wt% betaine in PAA 1%, pH=5	Yes	45.46	$2.94 \cdot 10^{-8}$	-33.2
0.1 wt% betaine in PAA 1%, pH=5, 2xPDADMAC 1% (2M NaCl)	No	30.67	$1.98 \cdot 10^{-8}$	+22.39

#### 4.3. PHMB adsorption on Vasolipid surface

In the sections below results from light microscopy and zeta-potentials measurement are presented.

##### 4.3.1. Light microscopy

Most of the Vasolipid spheres were smaller than  $1\mu\text{m}$  and they were not clearly visible in figure 20. They were visible with the microscope; however, they moved too fast in solution to be captured in an images. The capsule in figure 20 is one among the larger spheres, but most of them were rather small.

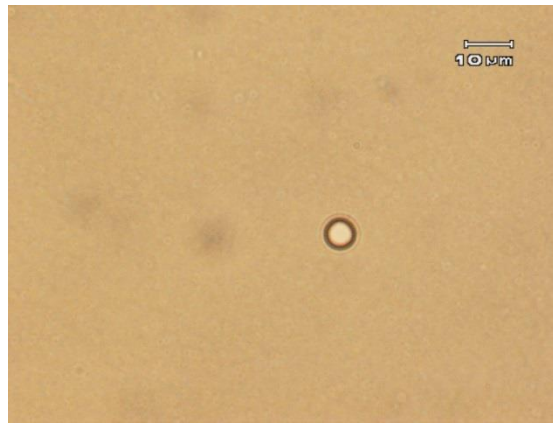


**Figure 20: Vasolipid capsules with PHMB adsorbed on the surface.**

### 4.3.2. Zeta-potential

The Vasolipid capsules were negatively charged and therefore highly cationic PHMB could adsorb on the surface. The adsorption increased the  $\zeta$  potential quite significantly to a positive value. These results are presented in table 3.

**Table 3: Zeta-potential measurement for Vasolipid and PHMB adsorbed on the vasolipid surface.**

Sample	Washed	Capsules velocity ( $\mu\text{m/s}$ )	Electrophoresis mobility ( $\text{m}^2/\text{V.s}$ )	Zeta-potential (mV)
<b>Vasolipid</b>	Yes	33.69	$2.18 \cdot 10^{-8}$	-24.73
<b>Vasolipid + PHMB 0.4 %</b>	No	57.88	$3.74 \cdot 10^{-8}$	+42.49
<b>Vasolipid + PHMB 0.4%</b>	Yes	61.16	$3.95 \cdot 10^{-8}$	+44.64
<b>Vasolipid + PHMB 0.4% + PLGA 1% and 1M salt</b>	Yes	Goes toward zero	-	Goes toward zero

When PLGA was added it did not seem capable of covering the whole capsule surface. PLGA could hence only compensate the surface charge of PHMB but not create an excess charge. Therefore the next layer of oppositely charged polyelectrolyte cannot be adsorbed on the surface.

## 4.4. Production of hollow multilayer capsules and loading with FITC-dextran

The results from all steps of production of hollow capsules, crosslinking and loading with FITC-dextran are presented below.

### 4.4.1. Light microscopy

Figure 22 illustrates  $\text{CaCO}_3$  with one layer, PAH 4mg/mL, and with an increased adsorption time than the original process had. The capsules were aggregated which is normal for spherical particles in solution, and was described by the producer of the calcium carbonate spheres. After 3 bilayers the capsules aggregated more, see figure 21, but they were still spherical which was considered to be ok.

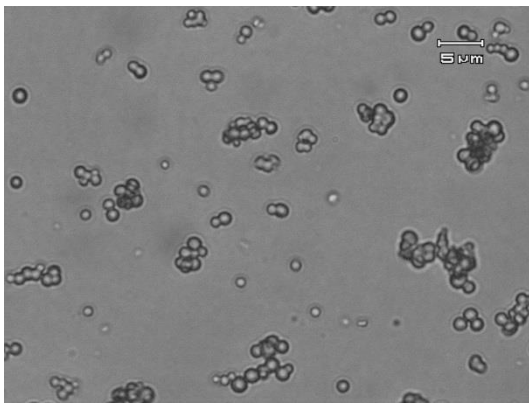


Figure 22:  $\text{CaCO}_3$  capsules with PAH 4mg/mL, longer adsorption time.

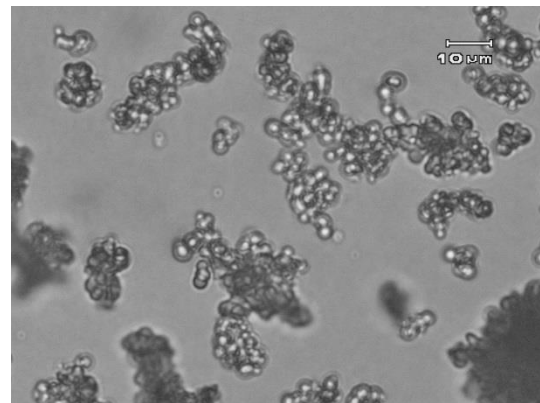


Figure 21:  $\text{CaCO}_3$  capsules with 3 bilayers (PAH/PLGA), polyelectrolyte concentration 4mg/mL, and longer adsorption time

With lower concentration of polyelectrolytes and a shorter adsorption time, the  $\text{CaCO}_3$  capsules aggregated more, see figure 24. After adsorption of 3 bilayers the capsules aggregated even more, see figure 23.

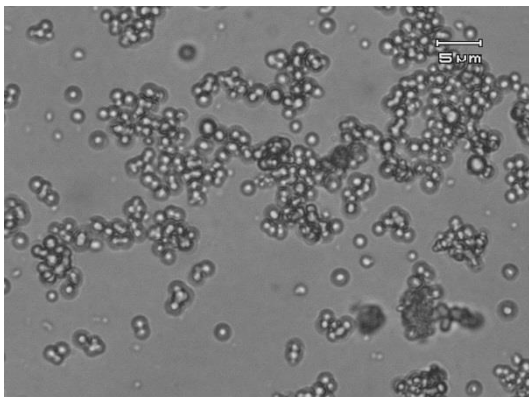


Figure 24:  $\text{CaCO}_3$  capsules with PAH 2mg/mL, shorter adsorption time

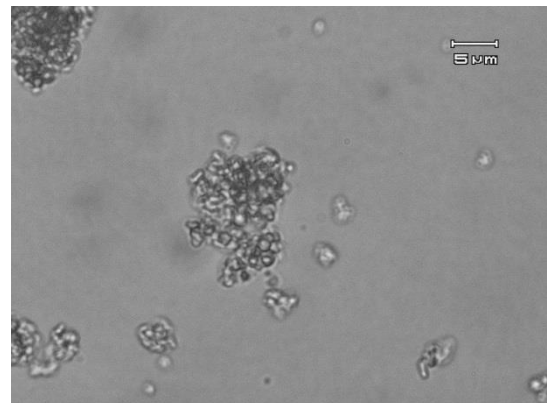
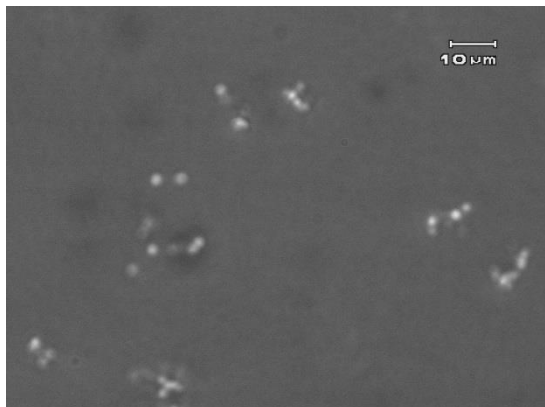


Figure 23:  $\text{CaCO}_3$  capsules with 3 bilayers (PAH/PLGA), polyelectrolyte concentration 2mg/mL, and shorter adsorption time



These images show that higher polyelectrolyte concentration and longer adsorption time was needed to get less aggregation and to preserve the stability of the  $\text{CaCO}_3$  capsules.



**Figure 26: Air dried hollow capsules cross-linked by 200mM EDC and 50mM sulfo-NHS**

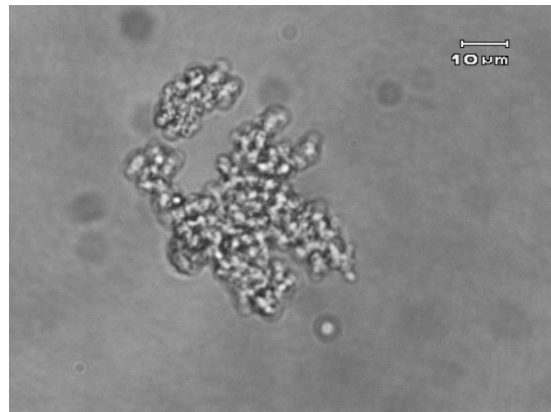


**Figure 25: Air dried hollow capsules cross-linked by 50mM EDC and 50mM sulfo-NHS**

Figures 25 and 26 demonstrate hollow capsules cross-linked by 200mM EDC and 50mM sulfo-NHS (figure 26), and 50mM EDC and 50mM sulfo-NHS (figure 25). Both of them were transparent, and it was clear that the light from the microscope went through the capsules, an indication that the core had been dissolved. The capsules cross-linked by 200mM EDC were more stable. They kept their form and were still spherical when they were dried, see figure 26. But those capsules cross-linked by 50mM EDC were more aggregated and they did not keep their spherical shape as well, see figure 25.

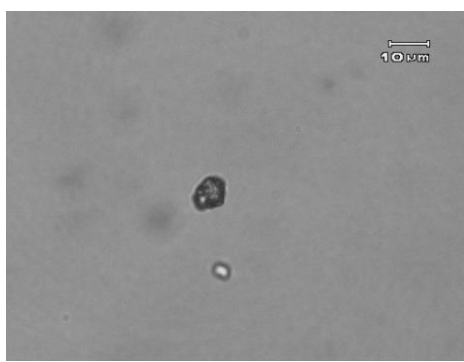


**Figure 27: Loaded capsules with FITC-dextran, exposed to V8.**

Hollow capsules were loaded with FITC-dextran and were exposed to V8 for one day. Light microscopy pictures show that the enzyme had been activated and degraded at least parts of the multilayer capsules and thus probably released the FITC-dextran. After break down of the capsules, mostly collections of polymer chains remained and only very few capsules were



present, which are shown in figure 27. This event indicates enzymatic activity of V8 on the glutamic acid bonds. Despite the size difference between PLGA and the very large PAH, the intermingling of polyelectrolytes in all directions seemed to expose glutamic acid bonds through the film enabling a structure change. However, these results are preliminary, and more work needs to be done to study the degradation properties.

#### 4.4.2. Zeta-potential measurements

The results of the zeta-potential measurements are presented in table 3 and figure 28. These measurements show that the multilayer surface has been charge-overcompensated in each adsorption step, *i.e.* promoting adsorption of the next oppositely charged polyelectrolyte.

Table 3: Zeta potential measurement for CaCO<sub>3</sub> multilayer capsules.

Sample	washed	Capsules velocity (μm/s)	Electrophoresis mobility(m <sup>2</sup> /V.s)	Zeta-potential (mV)
CaCO <sub>3</sub> +PAH	Yes	18.57	1.2*10 <sup>-8</sup>	+13.55
CaCO <sub>3</sub> +PAH+PLGA	Yes	31.13	2.02*10 <sup>-8</sup>	-22.86
CaCO <sub>3</sub> +PAH+PLGA+PAH	Yes	16.42	1.06*10 <sup>-8</sup>	+11.98
CaCO <sub>3</sub> +PAH+PLGA+PAH+PLGA	Yes	41.85	2.7*10 <sup>-8</sup>	-30.55
CaCO <sub>3</sub> +PAH+PLGA+PAH+PLGA+PAH	Yes	38.89	2.51*10 <sup>-8</sup>	+28.39
CaCO <sub>3</sub> +PAH+PLGA+PAH+PLGA+PAH+PLGA	Yes	63.2	4.08*10 <sup>-8</sup>	-46.13

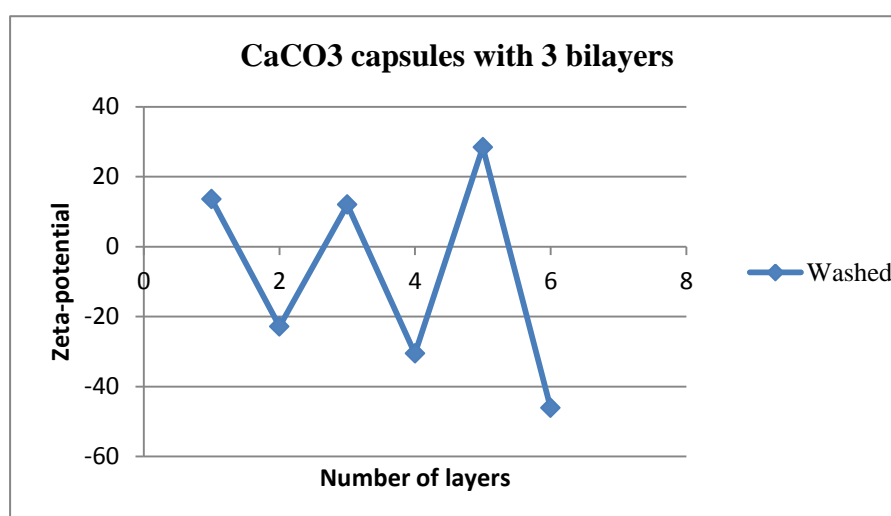
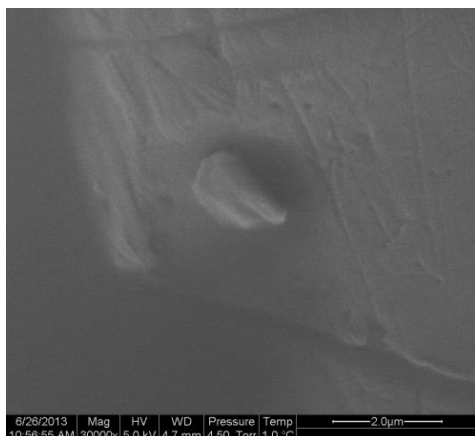


Figure 28: Zeta-potential measurements for multilayers on CaCO<sub>3</sub> capsules.

#### 4.4.3. ESEM images

Hollow capsules were investigated in ESEM, see figure 29 and 30. When water evaporated in the ESEM instrument (because of the low pressure) the capsules collapsed and crevices seemed to occur on the wall, see figure 30.



**Figure 29: Hollow capsule in the ESEM instrument during water evaporation (dark area is water)**

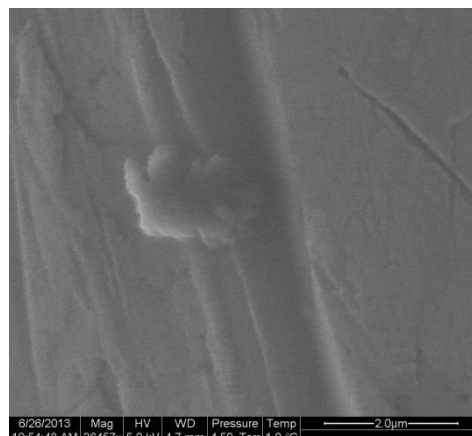


**Figure 30: Hollow capsule in ESEM instrument when water has evaporated.**

When water evaporated, the capsules were deformed and became flatter, see figure 29, which was proof of  $\text{CaCO}_3$  core removal. There was still water on the left side of the droplet in figure 29, and the capsule remained spherical at this side. But when water had evaporated completely from the surroundings, the flat capsule had ruptured, see figure 30. This behavior was probably not only due to the drying process itself, but also because of the very low pressure and the slightly destructive electron beam in the ESEM environment.

#### 4.4.4. SEM images

The  $\text{CaCO}_3$  capsules' multilayers were cross-linked with 200mM EDC and 50mM sulfo-NHS, and then air dried before sputtering the surface with gold. The sample was investigated in SEM and the result is presented in figure 31. The capsules were spherical, since the  $\text{CaCO}_3$  core still was present, see figure 32.

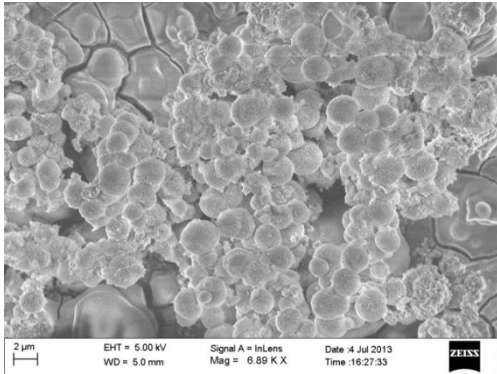


**Figure 32: CaCO<sub>3</sub> capsules' multilayers that were cross-linked with 200mM EDC and 50mM sulfo-NHS, and then air dried.**

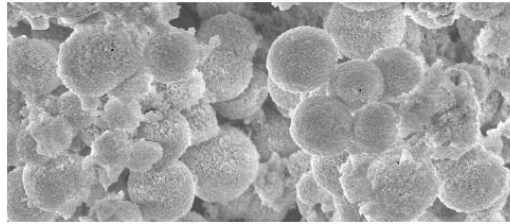


**Figure 31: A close-up of the capsule surface.**

The capsules in figure 32 display a smoother surface between each sphere, almost connecting the capsules to each other. This could indicate an interaction between multilayers between each capsule.

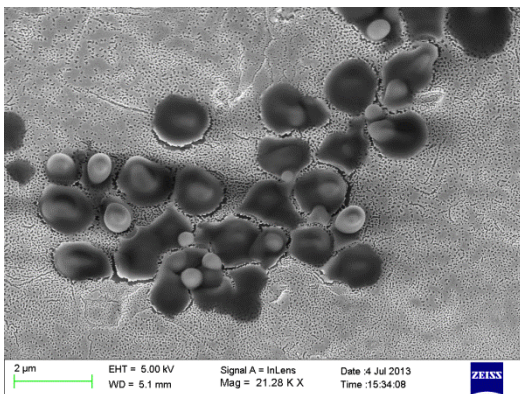


**Figure 33: Hollow capsules cross-linked by 200mM EDC and 50mM sulfo-NHS, freeze-dried.**

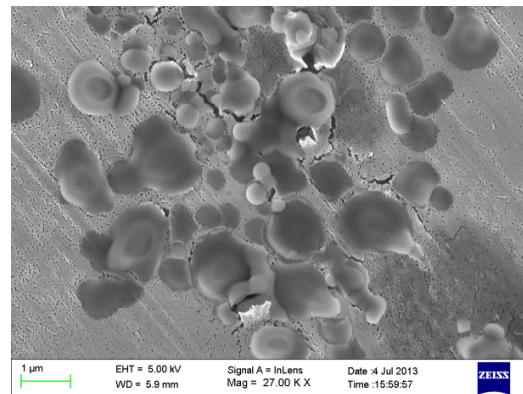


**Figure 34: Hollow capsules cross-linked by 200mM EDC and 50mM sulfo-NHS, air-dried.**

Figure 33 and 34 illustrate hollow capsules cross-linked with 200mM EDC and 50mM sulfo-NHS, which were freeze-dried and air dried, respectively. The darker spots are capsules on the bottom, in direct contact with the sample holder, and the slightly brighter spots seemed to be capsules that had aggregated on top of the other spheres. The capsules were flattened to different degrees after either freeze or air drying. Those closest to the bottom were flatter and more elongated, possibly due to interactions between the capsules and the sample holder. The capsules that were further away from the holder remained spherical in vacuum. The capsules that were freeze-dried seemed to retain their structure more (in general) than the air dried capsules.

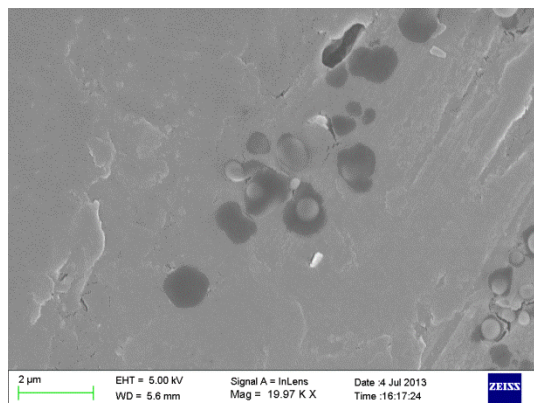


**Figure 35: Hollow capsules cross-linked by 50mM EDC and 50mM sulfo-NHS, air dried.**

Hollow capsules crosslinked by 50mM EDC and 50mM sulfo-NHS were air dried and are shown in figure 35. Since the multilayers were less crosslinked, it was no surprise that these capsules retained their structure to a lesser degree than the more crosslinked ones. In other words, they were more easily deformed.

#### **4.4.5. CLSM on loaded capsules**

Hollow capsules cross-linked with either 50mM EDC or 200mM EDC (and 50 mM sulfo-NHS) and then loaded with FITC-dextran (MW=4000) in the core. The FITC-dextran was used as a model substance for PHMB (MW=3000). Either 0.15M NaCl or 0.5M NaCl was used as a means to promote core loading by screening of multilayer charges. The results are presented in figures 36-39. There were no apparent changes detected when the salt concentration was changed, since all capsules were successfully loaded with FITC-dextran; however, the multilayers crosslinked with 200mM EDC seemed to aggregate less with 0.5M NaCl. As expected, the capsules cross-linked by 50mM EDC and 50mM sulfo-NHS shrunk more than the 200mM capsules, due to a softer and more deformable structure since they were less crosslinked, see figures 36-37.



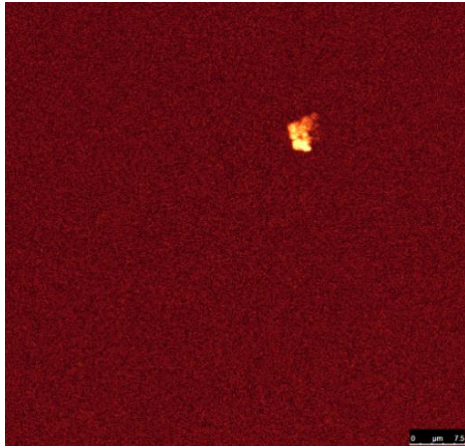


**Figure 36:** Hollow capsules cross-linked with 50mM EDC and 50mM sulfo-NHS, loaded with FITC-dextran in 0.5M NaCl.

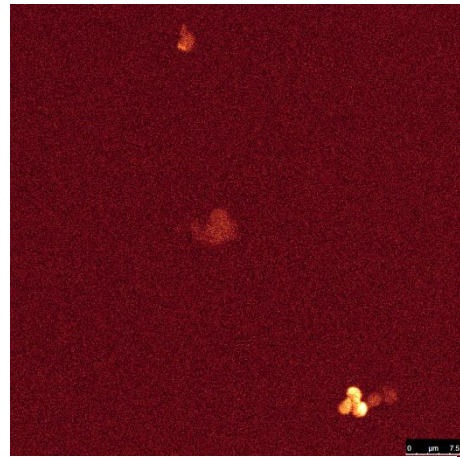


**Figure 37:** Hollow capsules cross-linked with 50mM EDC and 50mM sulfo-NHS, loaded with FITC-dextran in 0.15M NaCl.

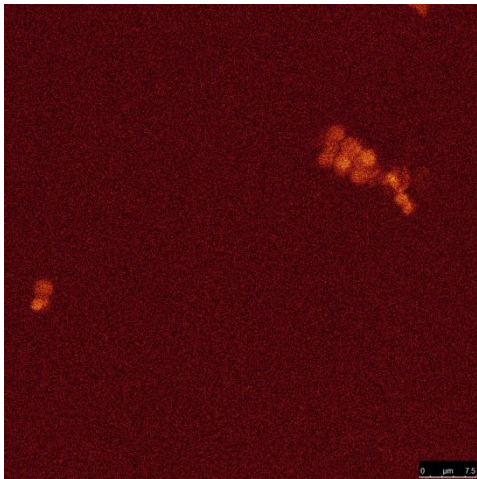


**Figure 38:** Hollow capsules cross-linked with 200mM EDC and 50mM sulfo-NHS, loaded with FITC-dextran in 0.5M NaCl.

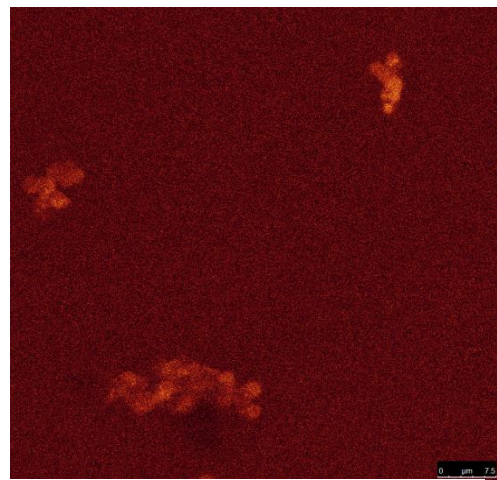


**Figure 39:** Hollow capsules cross-linked with 200mM EDC and 50mM sulfo-NHS, loaded with FITC-dextran in 0.15M NaCl.

The hollow capsules cross-linked with 200mM EDC and 50mM sulfo-NHS and then loaded with FITC-dextran in 0.5M NaCl were exposed to V8 at 32°C and 37°C. No changes were detected in the CLSM, see figures 40-43, *i.e.* no enzymatic degradation is shown in the present system. However, capsules were left overnight with V8 for further studies in the light microscope. The light microscopy images contradicted the CLSM results, see figure 27, and could possibly be due to differences in volume (Several ml compared to 7  $\mu$ l) or time of exposure to the V8 enzyme.

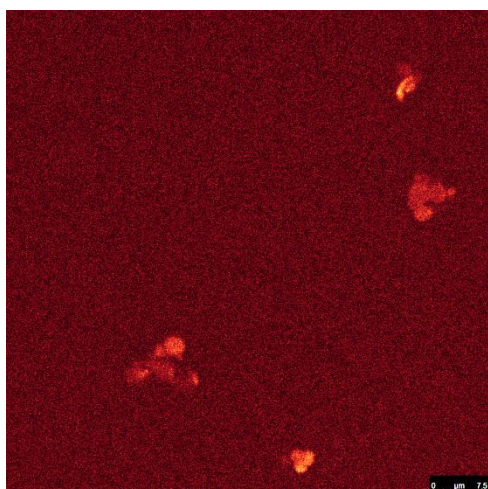


Figure 41: Loaded capsules, exposed to V8 at 32°C, from start.

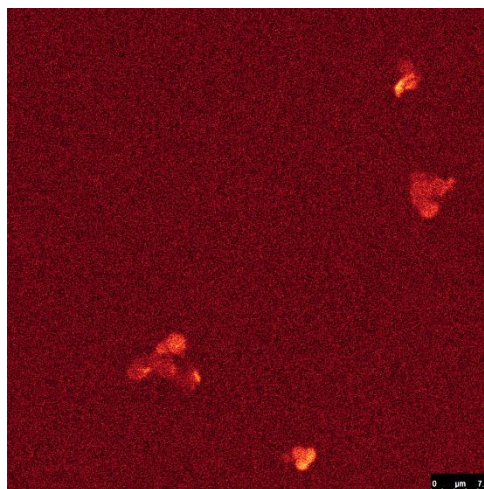


Figure 40: Loaded capsules, exposed to V8 at 32°C, after a while

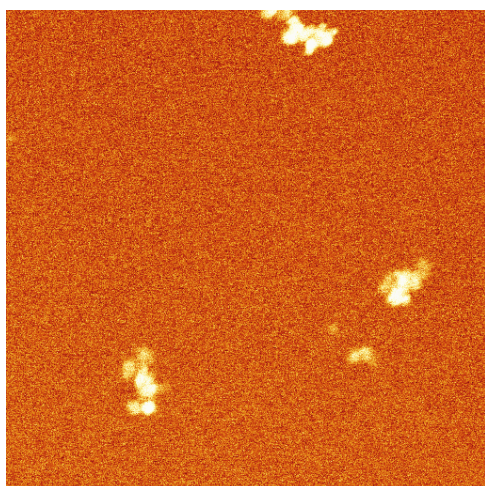


Figure 43: Loaded capsules, exposed to V8 at 37°C, after a while.

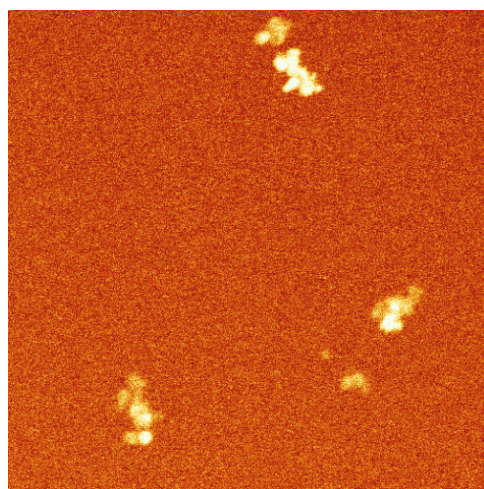


Figure 42: Loaded capsules, exposed to V8 at 37°C, from start.

## 5. Discussion

PLGA and PLL were the main polyelectrolytes when forming capsules. Betaine ester was dissolved in glyceryl trioctanoate and used as the core in an o/w emulsion with PLGA as emulsifier. Different amounts of betaine ester were dissolved in glyceryl trioctanoate, and the optimum amount was found to be 0.1 wt%. Due to the high cost of PLGA and PLL, PAA and polyDADMAC were used as substitutes. It was expected that PAA and polyDADMAC would work just as well as PLGA and PLL, but this was not the case.

PAA and polyDADMAC proved to need a higher NaCl and polyelectrolyte concentration than PLGA and PLL when producing the o/w emulsion that was the starting point for capsule production. Even though higher concentrations of NaCl- and PAA/polyDADMAC proved to

give slightly better results, the o/w emulsion was not stable. The pH was varied as a last resort; however, this did not improve the stability of the emulsion. The oil-spheres aggregated when increasing the polyelectrolyte concentration, possibly due to hydrophobic interaction. The water soluble betaine ester may also have a tendency to diffuse out to the water phase, which could contribute to the instability of the emulsion. When polyDADMAC was added, complexes were formed during the filtration. A probable reason could have been that PAA and the oil phase was a poor match, hence favoring the formation of complexes with polyDADMAC instead. Another more far-fetched interaction could be that polyDADMAC may bind to the carboxyl group of glyceryl trioctanoate and form a complex.

When the emulsion with PAA/polyDADMAC was filtrated it seemed to be glued to the filter paper despite the paper's "low adsorbing protein" property.

PLGA and PLL are naturally occurring polyelectrolytes. They are also biocompatible and biodegradable, which favor them for use in drug delivery. The optimum NaCl concentration, when using these polyelectrolytes, was 0.1M. Higher NaCl concentration weakens the electrostatic interaction present between PLGA and PLL and causes disruption of the polyelectrolyte multilayer (39). After every added layer the emulsion was centrifuged and washed twice, but complexes were formed every time. The polyelectrolytes could not withstand being washed twice (10 000 rpm for 1.5 hours) and the core leaked out. However, when only washing the emulsion once, the emulsion remained stable. The optimum concentration and amount of everything for producing emulsion was found to be:

- 0.1 wt% betaine ester was dissolved in glyceryl trioctanoate
- Either PLGA or PLL in an amount corresponding to 1 mg/mL
- 0.1M NaCl
- 0.1mM Tris-HCl
- pH=7.4

When the emulsion was left on a magnetic stirrer it was stable for a while, at least 1 month. However, the larger capsules consistently leaked until rupturing completely, which was seen as an oil-phase on top of the emulsion. Consequently, the emulsion can be kept stable for a couple of months, unless strengthening the multilayer structure with *e.g.* crosslinking. However, the enzyme should still be able to break down the partially crosslinked multilayers and release the active substance. The added chemicals should also be biocompatible and biodegradable to minimize the side-effects on the human body.



Zeta-potential measurements showed different values before and after washing, since the excess polyelectrolytes were removed during the wash step. According to literature (11) multilayers have a “fuzzy” structure and can diffuse out between layers. The results from the zeta-potential measurements confirm this, as the values differ slightly between measurements since every layer was unique.

When the emulsion with PLGA/PLL was air dried, the capsules collapsed. They seemed to have vanished when studying them in the light microscope, which probably means that they could not withstand air drying due to fractures and leakage. However, when they were crosslinked with EDC and sulfo-NHS, ESEM results showed that the stability of the capsules was increased. This was expected since the structure of the shell becomes more rigid after crosslinking, and even though air drying flattened the capsules and made them smaller (shrinkage), they were still visible in ESEM and in the light microscope. It is difficult to say whether V8 can manage to break down the multilayer when it is crosslinked, but this needs to be tested in the future.

PHMB was adsorbed on Vasolipids capsules, this is shown by the zeta-potential measurements. Anionic PLGA was then added to adsorb on top of the PHMB, but the zeta-potential measurements showed that the surface potential now was close to zero. The reason could have been that PLGA was not able to cover the whole surface due to PHMB's inability to create multilayers. In other words, PHMB's strong cationic character may have created a situation where the weak polyelectrolyte (PLGA) was not able to overcompensate the surface charge. This could easily be tested with a different anionic than PLGA; however, this was not tested due to time constraints.

When the multilayers were built up on the  $\text{CaCO}_3$  template, the adsorption times and the polyelectrolyte concentrations had to be increased. Under these conditions, the capsules became much more stable. They did not aggregate as much as when the adsorption time was shorter and the polyelectrolyte concentration was lower. They also retained their spherical shape better after core removal and after adsorbing 3 bilayers. Also, the high molecular weight cation PAH (non-biodegradable) was used as a model substance in these studies.

The hollow capsules cross-linked with 200mM EDC and 50mM sulfo-NHS were more stable than using 50mM EDC and 50mM sulfo-NHS. This was expected due to the higher degree of crosslinking with more EDC, which creates a more rigid shell that prevents deformation.



The results of the zeta-potential measurements were unfortunately not reliable throughout the CaCO<sub>3</sub> capsule making; however, in figure 28 the only reliable measurement is presented. The instrument was found not to be working correctly and could not be fixed before this project's end.

ESEM images showed that the cross-linked capsules collapsed as the water evaporized at 1° C and low pressure. Cracks appeared on the edges as water disappeared and the capsules were flattened.

The SEM measurements illustrated that the capsules closest to the sample holder were flattened and elongated, while the other capsules above them partially retained their spherical shape. Interaction between the holder and the capsules may have been the reason for this. The capsules that were freeze-dried were more stable, given that the capsules had been cross-linked with 200mM EDC and 50mM sulfo-NHS.

From the ESEM and the SEM measurements it was concluded that core removal with GDL had been successful, since the capsules were deformed when dried compared to the fine spherical capsules that existed before CaCO<sub>3</sub> dissolution. Also, 200mM EDC was needed to stabilize the shell structure to allow drying of the capsules, but it may be necessary to increase the crosslinking degree further.

With CLSM the possibility of loading the capsules with a rather high molecular weight substance (FITC-dextran, MW = 4000) was studied. The pictures showed instantly that the loading had been successful. At first, there were no apparent differences with loading capacity when using different NaCl-concentrations. Later on it was discovered that the higher salt concentration contributed to less aggregation of the capsules with the higher crosslinking degree, and also the intensity of the same sample was slightly higher than for the sample with less salt. The capsules cross-linked by 50mM EDC had shrunk but those cross-linked by 200mM EDC seemed to have maintained the spherical form better. These results concluded that a higher crosslinking degree was necessary to create a stable capsule, and the higher NaCl concentration was needed for proper loading and for aggregation issues. The capsules with a higher degree of crosslinking were exposed to V8 at 32°C and at 37°C but no degradation was detected in the CLSM., *i.e.* no signs of V8 breaking down the multilayer and releasing FITC-dextran. V8 may not have been able to break down the multilayers since PAH not is biodegradable, but the partial crosslinking could also have been a limiting factor. However, time and the small volume used in the CLSM seemed to affect the degradation. The remaining

parts of the sample had V8 added to it and then it was stored overnight before light microscope studies. The images now showed dark thread-like clusters of polymer chains instead of capsules or aggregates of capsules. These images showed that V8 had been active and degraded parts of the multilayer. As previously explained, the polyelectrolyte film is a “fuzzy” construction, with polymer chains in all directions. Despite the size difference of PAH and PLGA, the available glutamic acid bonds may have been enough for V8 to completely change the capsule structure by enzymatic degradation of PLGA. To shed light on the matter further more studies are needed.

PLGA was chosen as the outermost layer. This is because PLGA is an anionic polypeptide and due to electrostatic repulsion between the negatively charged cell surface and the polymer the cellular uptake of the polymer is hindered (22). A study (12) has shown that the detachment forces between cells and polyelectrolytes are much higher on PLL-ending films than PLGA-ending film. This is probably accurate for multilayer capsules too. Lower detachment forces are desired for wound dressings. When a wound dressing is removed with a high detachment force, cells are pulled off along with the wound dressing. It happens that the wound opens again and even starts to bleed, therefore a low detachment force is among the more desired properties of a wound dressing and for anything that is incorporated in it.

## 6. Future work

Future research for the o/w emulsion capsules could look into testing pH, pressure and temperature combinations to find out if the capsules can be stabilized further. The stability can also be improved by adding other biocompatible, biodegradable, and preferably naturally occurring, compounds. However, this compound should not affect the enzymatic degradation process of the multilayer.

PLGA could not overcompensate the charge of PHMB and cover the surface to create multilayers. A different polymer, preferably naturally occurring, can be tested to build up multilayers on PHMB.

Another possible future study could test if the porous  $\text{CaCO}_3$  templates can be loaded with active substances and still assemble a multilayer on the template. Important is that the surface charge of the template does not change too much to enable build-up of a multilayer.

## 7. Acknowledgement

I would like to thank my examiner, Professor Krister Holmberg for all his help and dedication during this project. I would also like to thank my supervisor, Marina Craig, for her help, knowledge and patience when teaching me to produce capsules. I thank her for encouragement and support that I got from her when the results from the samples were not as expected. I am grateful to Mölnlycke Health Care for economic support. Finally, I would like to thank Dr. Erich Schuster from SiK for running the CLSM, Anna Jansson for ESEM measurements, Tina Gschneidner for SEM measurements, and all personnel at Applied Surface Chemistry, especially Dr. Markus Andersson Trojer who helped me a lot with the o/w emulsion procedure and Jonathan Borg who helped me with the light microscope.

## References

1. **Kirketerp-Møller, Klaus, Zulkowski, Karen och James, Garth.** Chronic Wound colonization, Infection and Biofilms. [bokförf.] T Bjarnsholt, C Moser och N Høiby. *Biofilm infection*. Koege : Springer Science+ Business Media, 2011, 2, ss. 11-24.
2. *The significance of surface pH in chronic wounds.* **wounds UK 2007.** 3, 2007, Wound healing science, Vol. 3, pp. 52-56.
3. *Staphylococcus aureus infection on cut wounds in the mouse skin: experimental staphylococcal botryomycosis.* **Hisanori, Akiyan; Hiroko, Kanzaki; Joji, Tada; Jiro, Arata.** 3, Okayama : Journal of Dermatol Science, Mach 1996, Sciencedirect, Vol. 11, ss. 234-238.
4. *Confocal laser microscopic observation of glycocalyx production by Staphylococcus aureus in vitro.* **Hisanori, Akiyama; W.K., Huh; Kazuyasu, Fuji; Osamu, Yamasaki; Takashi, Oono; Keiji, Iwatsuki.** 1, Okayama : Journal of Dermatol Science, May 2002, Vol. 29, ss. 54-61.
5. *Assessment of Streptococcus pyogenes microcolony formation in infected skin by confocal laser scanning microscopy.* **Hisanori, Akiyama; Shin, Morizane; Osamu, Yamasaki; Takashi, Oono; Keiji, Iwatsuki.** 3, Okayama : Journal of Dermatol Science, September 2003, Vol. 32, ss. 193-199.
6. *Understanding biofilm resistance to antibacterial agents.* **Davies, David.** 2, New York : Nature Reviews Drug Discovery, February 2003, Vol. 2, ss. 114-122.
7. *Biofilm in chronic wounds.* **James, Garth A; Swogger, Ellen, Wolcott, Randall; Pulcini, Elinor; Secor, Patrick; Sestrich, Jennifer; Costerton, John W; Stewart, Philip S.** 1, u.o. : Wound Repair And Regeneration, January-February 2008, Vol. 16, ss. 37-44.
8. *Polypeptide multilayer self-assembly and enzymatic degradation on tailored gold surfaces studied by QCM-D.* **Craige, Marina; Bordes, Romain; Holmberg, Krister.** 8, Gothenburg : The Royal Society of Chemistry, 2012, Soft Matter, pp. 4788-4794.
9. *Zipper-like properties of [poly(L-lysine) + poly(L-glutamic acid)]  $\beta$ -pleated molecular self-assembly.* **Dzwolak, Wojciech; Marszalek, Pitor E.** 44, s.l. : Chemical Communication, 2005, chem. commun., pp. 5557-5559.
10. *Immobilization of Enamel Matrix Derivate Protein onto Polypeptide Multilayer. Comparative in Situ Measurement Using Ellipsometry, Quartz Crystal Microbalance with Dissipation, and Dual-Polarization Interferometry.* **Halthur, Tobias J; Claesson, Per M.; Elofsson, Ulla M.** 26, Stockholm : American Chemical Society, 2006, Langmuir, Vol. 22, pp. 11065-11071.
11. *Multilayers of Charged Polypeptides As Studied by in Situ Ellipsometry and Quartz Crystal Microbalance with Dissipation.* **Halthur, Tobias J.; Elofsson, Ulla M.** 5, Stockholm : American Chemical Society, 2004, Langmuir, Vol. 20, pp. 1739-1745.
12. *pH dependent growth of poly(L-lysine)/poly(L-glutamic) acid multilayer films and their cell adhesion properties.* **Richert, Ludovic; Arntz, Yuri; Schaaf, Pierre; Voegel, Jean-Claude; Picart, Catherine.** 1-2, Stranbourg : Science Direct, 2004, Surface Science, Vol. 570, ss. 13-29.

13. **Decher, Gero; Schlenoff, Joseph B.** *Multilayers Thin Films*. s.l. : WILEY-VCH Verlag GmbH & Co. KGaA, Weinheim, 2003. ISBN 3-527-30440-1.
14. **Kickelbick, Guido.** *Hybrid Materials: Synthesis, Characterization, and Applications*. Wien : WILEY-VCH Verlag GmbH & Co. KGaA, 2007. pp. 28-29. 978-3-527-61048-8.
15. *Theory of polyelectrolytes in solutions and at surfaces.* **Dobrynin, Andrey V.; Rubinstein, Michael.** 11, s.l. : Progress in polymer science, 2005, Vol. 30, pp. 1049-1118.
16. **W, John; CA, Buckley; EP, Jacobs; RD, Sanderson.** *Synthesis and use of polyDADMAC for water purification*. Durban : Conference Planners, 2002. ISBN 1-86845-844-X.
17. Chemistry beyond the ordinary. *polysciences*. [Online] polysciences, Inc., 2013. <http://www.polysciences.com/Catalog/Department/Product/98/categoryid--298/productid--2641/>.
18. *Dispersion and Film-Forming Properties of Poly(acrylic acid)-Stabilized Carbon Nanotubes.* **Saint-Aubin, Karell; Poulin, Philippe; Saadaoui, Hassan; Maugey, Maryse; Zakri, Cécile.** 22, Pessac : American Chemical Society, 2009, Langmuir, Vol. 25, ss. 13206-13211.
19. *Aqueous polyacrylic acid based gels: physicochemical properties and applications in cultural heritage conservation.* **Carretti, E; Dei, L; Baglioni, P.** Florence : Springer-verlag, 2004, Vol. 123, ss. 280-283.
20. *Understanding the fundamentals of polypeptides and proteins.* **Hu, Gary.** 1, California : u.n., BioProcessing journal, Vol. 10, ss. 12-14.
21. Student Resources for General Chemistry. *Chemed*. [Online] Chemed DL. (<http://chemed.chem.wisc.edu/chempaths/GenChem-Textbook/Polypeptide-Chains-1024.html>).
22. *Poly(L-glutamic acid)-anticancer drug conjugates.* **Li, Chun.** 5, Houston : Advanced Drug Delivery Reviews, September 2002, Advanced drug delivery reviews, Vol. 54, ss. 695-713.
23. *Water-soluble graphene covalently functionalized by biocompatible poly-L-lysine.* **Shan, Changsheng; Yang, Huafeng; Han, Dongxue; Zhang, Qixian; Ivaska, Ari; Niu, Li.** 20, u.o. : American Chemical Society, 2009, Langmuir letter, Vol. 25, ss. 12030-12033.
24. *Aggregation Processes of a Weak Polyelectrolyte, Poly(allylamine) Hydrochloride.* **Park, Jaejung; Choi, Young-Wook; Kim, KyungBae; Chung, Hoeil; Sohn, Daewon.** 1, u.o. : Bull. Korean Chem. Soc., 2008, Vol. 29.
25. **Ahlström, B.** *Quaternary ammonium esters as soft antimicrobial agent*. Gothenburg : u.n., 1999.
26. *Antimicrobial Activity of Betaine Esters, Quaternary Ammonium Amphiphiles Which Spontaneously Hydrolyze into Nontoxic Components.* **LINDSTEDT, M.; ALLENMARK, S.; THOMPSON, R. A.; EDEBO, L.** 10, Gothenburg : American Society for Microbiology, 1990, Vol. 34, ss. 1949-1954.
27. *Microbial growth and accumulation in industrial metal-working fluids.* **Mattsby-Baltzer, I; Sandin, M; Ahlström, B; Allenmark, S; Edebo, M; Falsen, E; Pedersen, K; Rodin, N; Thompson, R. A.; Edebo, L.** 10, u.o. : Applied and Environmental Microbiology, October 1989, Vol. 55, ss. 2681-2689.

28. *Factors influencing the micellar catalyzed hydrolysis of long chain alkyl betainates.* **Thompson, Richard A och Allenmark, Stig.** 1, Gothenburg : Journal of Colloid and Interface Science, January 1992, Vol. 148, ss. 241-246.
29. *Reduced cytotoxicity of polyhexamethylene biguanide hydrochloride (PHMB) by egg phosphatidylcholine while maintaining antimicrobial efficacy.* **Müllera, Gerald; Kramera, Axel; Schmittb, Jürgen; Hardenb, Daniela; Koburgerc, Torsten.** 2-3, 2011 : Chemico-Biological Interactions, Vol. 190, ss. 171-178.
30. Polyhexamethylene Biguanide (PHMB). *archchemicals*. [Online] April 2008.
31. *Characterization of the glutamyl endopeptidase from Staphylococcus aureus expressed in Escherichia coli.* **Nemoto, Takayuki K; Ohara-Nemoto, Yuko; Ono, Toshio; Kobayakawa, Takeshi; Shimoyama, Yu; Kimura, Shigenobu; Takagi, Takashi.** 3, Nagasaki : Metapontum Agrobios., 2008, The FEBS Journal, Vol. 275, ss. 573-587.
32. **Stennicke, Henning R.; Breddam, Klaus.** Glutamyl Endopeptidase. [red.] Neil D Rawlings och Guy S Salvesen. *Handbook of proteolytic enzymes*. 3rd. Copenhagen : Academic press in an imprint of Elsevier Ltd, 2013, Vol. 1, 561, ss. 2534-2538.
33. **Cademartiri, Ludovico; Ozin, Geoffrey A.** *Concepts os Nanochemistry*. u.o. : WILEY-VCH Verlag GmbH & Co. KGaA. Weinheim, 2009. s. 236.
34. **Schweitzer, Jim.** Purdue university. *Radiological & environmental management*. [Online] 2010. <http://www.purdue.edu/rem/rs/sem.htm>.
35. **Knowles, W. Ralph, Schultz, William G. och Armstrong, Allen E.** *Environmental scanning electron microscope*. 5,362,964 United States, den 8 November 1994.
36. *Visualization of Food Structure by Confocal Laser Scanning Microscopy (CLSM).* **Durrenberger, Markus B.; Handschin, Stephan; Conde-Petit, Beatrice; Escher, Felix.** 1, u.o. : LWT - Food Science and Technology, February 2001, Vol. 34, ss. 11-17.
37. *pH-dependent thickness behavior of sequentially adsorbed layers of weak polyelectrolytes.* **Shiratori, S. S.; Rubner, M. F.** 11, u.o. : American Chemical Society, 2000, Vol. 33, ss. 4213-4219.
38. *Effect of pH.* u.o. : The Royal Society of Chemistry, 2011. Electronic Supplementary Material (ESI) for Soft Matter.
39. *Advances in polyelectrolyte multilayer nanofilms as tunable drug delivery systems.* **Jiang, Bingbing; Barnett, John B.; Li, Bingyun.** u.o. : Dove medical Press Ltd., August 2009, Nanotechnology, Science and Applications, Vol. 2, ss. 21-27.
40. Sigma Aldrich. *Sigma Aldrich*. [Online] Sigma-Aldrich Co LLC., 2013. <http://www.sigmaaldrich.com/catalog/product/aldrich/447013?lang=en&region=SE>.
41. Sigma Aldrich. *Sigma Aldrich*. [Online] Sigma-Aldrich Co LLC., 2013. <http://www.sigmaaldrich.com/catalog/product/sigma/p6282?lang=en&region=SE>.

42. Sigma Aldrich. *Sigma Aldrich*. [Online] Sigma-Aldrich Co LLC., 2013.  
<http://www.sigmaaldrich.com/catalog/product/aldrich/283223?lang=en&region=SE>).

43. kingnod group. *kingnodchem*. [Online] kingnod group Co., Ltd.  
<http://www.kingnodchem.com/phmb.asp>.

44. *Layer-by-layer self-assembly in the development of electrochemical energy conversion and storage devices from fuel cells to supercapacitors*. **Xiang, Yan; Lua, Shanfu; Jiang, San Ping**. 41, u.o. : Royal Society of Chemistry, 2012, *Layer-by-layer self-assembly in the development of electrochemical energy conversion and storage devices from fuel cells to supercapacitors*, ss. 7291-7321. 207890.